

Influence of Fatty Acid Methyl Ester Composition, Acid Value, and Water Content on Metallic Copper Corrosion Caused by Biodiesel

José G. Rocha Jr.,^a Marcelle D. R. dos Santos,^b Fernanda B. Madeira,^a
Sheisi F. L. S. Rocha,^a Glauco F. Bauerfeldt,^a Willian L. G. da Silva,^c
Acácia A. Salomão^c and Matthieu Tubino^{b,*c}

^a*Instituto de Química, Universidade Federal Rural do Rio de Janeiro,
BR-465, km 7, 23897-000 Seropédica-RJ, Brazil*

^b*Departamento de Engenharia Química, Universidade Federal Rural do Rio de Janeiro,
BR-465, km 7, 23897-000 Seropédica-RJ, Brazil*

^c*Instituto de Química, Universidade Estadual de Campinas, CP 6154,
13083-970 Campinas-SP, Brazil*

Oxidative stability parameters (OSP), acid value (AV), water content (W), and the metallic copper corrosion rate in biodiesels obtained from eight different vegetable oils were determined. Simple and multiple linear regression models were constructed to explain the influence of the OSP, AV and W variables on the corrosion rate. The corrosion rate was lower in biodiesel with less oxidative stability because, instead of reacting with copper, O₂ reacted preferentially with the unsaturated fatty acid methyl esters (FAME) that could act as “sacrificial molecules” to protect the copper against corrosion. Therefore, the corrosion rate was strongly related to the FAME composition. The AV was an important parameter in the corrosion process because free acids react with passivating agents, increasing the corrosion rate. The predictive capacity of W for corrosion rate was statistically insignificant, although water condensed on a copper surface causes corrosion.

Keywords: oxidative stability, corrosion, multiple linear regression, unsaturated FAME

Introduction

Biodiesel is currently an excellent alternative vehicle fuel for sustainability. It can be used in pure form or mixed in any proportion with diesel, forming a diesel-biodiesel binary mixture.^{1,2} Usually, diesel-biodiesel blends with low volume percent biodiesel are used in diesel engines. In some countries, such as the United States, Australia and Indonesia, this percentage reaches 20% (B20).³⁻⁵ The European Standard EN 16709⁶ specifies requirements and test methods for B30 marketed and delivered for use in diesel engines that are specially designed or adapted. However, in other countries, as in Brazil, this percentage is only 10% (B10).⁷ This is due, among other reasons, to the incompatibility of materials that make up the fuel circuit of diesel engines.⁸

Despite the advantages of biodiesel over diesel, biodiesel is significantly more susceptible to degradation, which often makes it more corrosive than diesel.^{8,9} The degradation

of biodiesel is mainly due to auto-oxidation reactions, moisture absorption, and the attack of microorganisms during the storage and use of biodiesel,^{10,11} and it may be more pronounced depending on the raw material as a consequence of differences in chemical composition, mainly in relation to the degree of instauration. The oxidation rate of biodiesel is more influenced by the composition of its alkyl esters than by environmental conditions (temperature, air, light, and the presence of metals).¹² A lower oxidative stability is obtained when a greater quantity of double bonds is present in the methyl ester. Allylic sites are especially susceptible to oxidation and bis-allylic sites are even more so. An allylic site shows a methylene CH₂ group adjacent to only one double bond. A methylene CH₂ group located between two double bonds is a bis-allylic site.¹³

In some studies on alkyl ester mixtures, oxidative stability was observed to depend strongly on the concentrations of linoleic and linolenic alkyl esters (polyunsaturated alkyl esters), rather than on the concentrations of saturated and monounsaturated alkyl esters, even if the latter are in greater proportion than the former in the biodiesel mixture. Most

*e-mail: tubino@iqm.unicamp.br

biodiesel fuels contain significant amounts of oleic (C18:1), linoleic (C18:2) or linolenic (C18:3) acid esters, that have 2 allylic sites and 0, 1, and 2 bis-allylic sites, respectively, decreasing the oxidative stability of the fuel. According to Knothe and Dunn, the relative rates of oxidation for these esters are 1 for oleates, 41 for linoleates, and 98 for linolenates.¹⁴

Short carbon chain acids formed at the end of biodiesel's degradation process, such as formic, acetic, propionic, and caproic acids, have been reported as responsible for the corrosion of the fuel supply system of the engine,^{10,13,15,16} suggesting that the biodiesel corrosiveness is inversely correlated with its oxidative stability. The corrosion of metals can trigger and catalyze other undesirable reactions leading to the instability and degradation of biodiesel,^{17,18} making it more corrosive. Reports can be found in the literature demonstrating the influence of the fatty acid methyl ester (FAME) composition on the oxidative stability of biodiesel, but not directly related to its corrosiveness.¹²⁻¹⁴ There is only a consensus that the corrosiveness of biodiesel is inversely proportional to its oxidative stability; however, this proposal is not supported by experimental data.

The presence of impurities, such as alcohol, free fatty acids (FFA), water, catalyst, and glycerol that remain at the end of the transesterification reaction was also reported as responsible for biodiesel corrosiveness.¹⁸ Additionally, as biodiesel is more hygroscopic than diesel, water can condense on the internal metal surfaces of the engine, favoring corrosion reactions and promoting microbial growth that causes additional corrosion.¹⁰

Copper is a component of the materials used for the production, storage, and transportation of biodiesel due to its excellent electrical and thermal properties, good mechanical workability, and good alloying ability. However, in biodiesel media, it easily undergoes corrosion, which undermined the long-term durability of piping and storage tanks.¹⁹ Besides, diesel engine parts like fuel pump, bearing, bushing, etc. are composed by copper alloy. Therefore, they are extensively influenced by corrosion occasionated by biodiesel.^{20,21} Sgroi *et al.*²² evaluated the corrosive effect of biodiesel on sintered bronze filter of an oil nozzle. The authors found that pitting corrosion occurred on bronze when the nozzle operated at 70 °C for several hours. Researchers observed that copper alloys are prone to be corroded by biodiesel compared to ferrous alloys and aluminum alloys.^{21,23}

Fazal *et al.*²⁴ reported that O₂, H₂O, CO₂, and RCOO• radicals dissolved in biodiesel are key factors that can affect its corrosiveness. They proposed a mechanism for the corrosion of metallic copper after performing a series of immersion tests on palm biodiesel at room temperature

(25-27 °C). These authors found that the oxidation of the metallic surface is done primarily by O₂, which produces Cu₂O and CuO. In presence of H₂O, Cu(OH)₂ is formed and, if CO₂ or RCOO• radicals are present, CuCO₃ is also produced. These solid compounds are formed on the metal surface constituting layers that protect the metal against posterior oxidation, reducing the corrosion rate. Therefore, the water and dissolved oxygen contents in the fuel are important factors that increase the corrosiveness of biodiesel, while RCOO• radicals and CO₂ act as inhibitors.

Aquino *et al.*²⁵ noted that the induction period (IP) of commercial biodiesel after the immersion at 55 °C of the copper and brass decreases from 8 to 0.05 h, revealing that the metallic ions present in the biodiesel, Cu²⁺ and Zn²⁺ ions, have a strong catalytic effect on the degradation reactions, regardless of the conditions of light and temperature and metallic ions concentration. Sarin *et al.*²⁶ have undertaken studies on stability of the neat *Jatropha* biodiesel in the presence of transition metals (iron, nickel, manganese, cobalt, and copper), likely to be present in the metallurgy of storage tanks and barrels. They found that influence of the metal was detrimental to oxidation stability and catalytic. Even small concentrations of metal contaminants showed nearly same influence on oxidation stability as large amounts. Copper showed the strongest detrimental and catalytic effect.

The objective of this work is to investigate the direct influence that the FAME composition exerts on biodiesel corrosiveness by measuring the mass loss of metallic copper plates after immersing them in biodiesels produced from different raw materials. Moreover, acid value (AV), water content (W), and some parameters associated to the oxidative stability of each biodiesel will be used for the construction of multiple linear regression (MLR) models in order to evaluate the relevance of these parameters in biodiesel corrosivity.

Experimental

Materials

For the synthesis of biodiesels, soybean, canola, linseed, sunflower, and corn oils were purchased in the local market. Macauba kernel oil was acquired from the Association of Small Scale Producers in the city of Riacho Dantas, Montes Claros, Minas Gerais, Brazil. Used frying oil was generously donated by the Environment Division of the University of Campinas. Palm kernel oil was acquired from the Agropalma company (Belém-PA, Brazil). Methanol, 99.8% purity, was supplied by Synth (Diadema-SP, Brazil) and 30% (m/m) sodium methoxide in methanol from

Vetec (Rio de Janeiro-RJ, Brazil) was used. For the final purification of the produced biodiesel Amberlite BD10 Dry, a sulfonic acid resin from Dow Chemical company (USA), was used. Thick electrolytic copper foils of 0.30 mm thickness were employed to perform corrosion tests. A mix of 14 fatty acid methyl ester standards, C8 to C24, was purchased from Supelco (Bellefonte, PA, USA). It was used for the confirmation of the retention time of each fatty acid methyl ester in the chromatograms.

Biodiesel synthesis

The synthesis of the biodiesels was performed in three steps. First, 16% (m/m) of methanol and 0.58% m/m of a methanolic solution of sodium methoxide (30% m/m) were mixed to the oil. The solution was maintained at 60 °C with mechanical stirring (900 rpm) for 1 h. Then, the reaction mixture was transferred to a separatory funnel for separation of the glycerin phase. In the second step, the upper phase was returned to the reaction flask, to which 4% (m/m) of methanol and 0.14% (m/m) of the catalyst solution were added (with respect to the initial mass of oil). The reaction was then carried out as in the first step.

In the third step, the biodiesel obtained in the second step was washed with five portions of water (50 mL) at 60 °C and then dried at 100 °C in an oven for 1 h. The biodiesel was then passed through a column containing Amberlite BD10 Dry resin to remove any impurities. In this scheme, 180 g of resin was employed *per* liter of biodiesel, and the percolation was performed at a flow rate of 4 mL min⁻¹.

For macauba, palm, and used frying oils, before performing the transesterification reaction, a prior step of FFA esterification was necessary. FFA are present in relatively high concentrations in these kinds of oils, which is evidenced by their high AVs. The esterification step was performed by adding, with respect to the initial mass of oil, 24% (m/m) of methanol and 1% (m/m) of concentrated sulfuric acid. The reaction mixture was heated at 50 °C and stirred at 900 rpm for one hour.

Analytical methods

The FAME composition of the biodiesel used for the experiments was determined using gas chromatography-mass spectrometry (GC-MS). An Agilent Technologies 5890A GC System (China) and Agilent Technologies 5975C inert XL MSD (China) with Agilent Technologies 7693 autosampler (China) were used under the following conditions: Agilent DB23 column (50% cyanopropyl-methylpolysiloxane) 30 m long, 0.25 mm internal

diameter, 0.25 µm film thickness; split injection 1:200; injection volume 1 µL; injector temperature 250 °C; initial temperature of the oven 60 °C, held for 1 min; 16 °C min⁻¹ heating rate up to 140 °C, held for 2 min; 0.5 °C min⁻¹ heating rate up to 150 °C; and 16 °C min⁻¹ heating rate up to 250 °C, held for 1 min; auxiliary oven at 250 °C. The mass spectrometer was operated with EI 70 eV (electron ionization), the solvent delay was 4 min, and the scanning range was 50-400 *m/z*. Peak identification was done by comparing the obtained mass spectra with those of the NIST11.L database and confirmed by comparing with the retention time of methyl ester standards. The quantitation was obtained through the normalization of the area under each chromatographic peak.

The induction period, IP, which expresses the oxidative stability, was determined in duplicate following the EN 14112 method,²⁷ using a model 873 Biodiesel Metrohm Rancimat (Switzerland).

The W was determined according to the EN ISO 12937 method,²⁸ using a model 831 KF Metrohm Karl Fischer coulometric titrator (Switzerland). The measurements were performed in triplicate.

The AV was determined following the method proposed by Aricetti and Tubino.²⁹ To perform the titration, a Metrohm Titrand 809 device (Switzerland) equipped with a Metrohm Solvotrode electrode (Switzerland) (electrolyte, saturated solution of LiCl in ethanol) and a Metrohm 814 USB Sample Processor (Switzerland) automatic sampler was used. All measurements were performed in duplicate.

Corrosion tests

Copper foil pieces (20 × 20 × 0.30 mm) were polished with SiC 420 and 220 grids sandpapers and subsequently sized with the aid of a caliper rule. According to ASTM G1-03 recommendations,³⁰ the copper foils were brushed with a nylon bristle brush, washed with distilled water, ethanol, and acetone, dried with hot air, and kept in a desiccator. The individual masses of the copper plates were determined on an analytical balance (± 0.00001 g). The washing and drying procedure was repeated for each piece until constant mass. Each copper plate was immersed, held suspended by a Nylon® thread, in 50 mL of biodiesel and maintained in an oven at 60 °C. On the sixth day, the biodiesels were submitted to vigorous stirring with a magnetic stir bar for 15 min. After that, the plates were maintained in an oven at 60 °C for more six days for a total of 288 h of immersion. The aim of the agitation was to promote the aeration of biodiesel replacing the oxygen consumed in the oxidation reactions. Otherwise, the corrosion rate may be low enough to hamper the mass loss measures.

The copper plates were then removed from the biodiesels, brushed, and washed with distilled water and ethanol. A solution of 10% (v/v) sulfuric acid was used to remove the corrosion products from the copper surface. The immersion time for pickling was 3 min. After the chemical treatment, the plates were washed with distilled water and acetone, dried with hot air, using a hair dryer, and finally weighed on an analytical balance. Cleaning procedures were also performed on copper plates to obtain the blank of corrosion rate. The water washing and drying procedures were repeated until constant mass. All assays were performed in triplicate. The average corrosion rate (in $\text{mg m}^{-2} \text{h}^{-1}$) was obtained using equation 1, as follows:

$$\text{corrosion rate} = (\Delta m \times 10^4) / (A \times t) \quad (1)$$

where: Δm is the loss of mass, in mg; A is the total area of the copper plate, in cm^2 ; t is the time of immersion, in h; and 10^4 is the conversion factor to convert cm^2 to m^2 .

Results and Discussion

Influence of FAME composition on corrosion rate

The corrosion rates of metallic copper are shown in Figure 1. According to these results, the biodiesel from used frying oil, macauba and palm kernel were the most corrosive among the studied biodiesels whereas those from canola, sunflower, and soybean oils presented relatively less corrosivity.

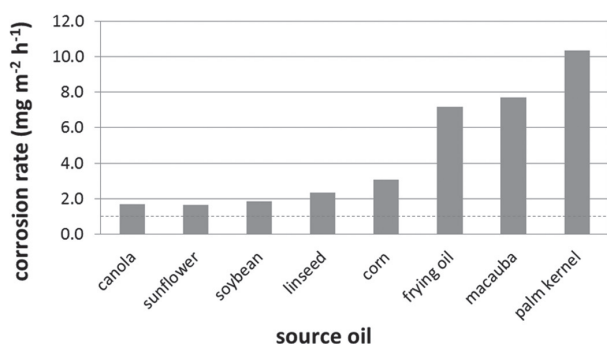


Figure 1. Corrosion rates on metallic copper immersed in biodiesel from different vegetable oils. The dotted line is the corrosion of the blank samples.

The compositional analysis in Table 1 revealed that the biodiesel corrosivity is related to the methyl esters of oleic (C18:1), linoleic (C18:2) and linolenic (18:3) acids, more specifically the level of unsaturated methyl esters. Soybean, sunflower, canola, linseed, and corn biodiesel were composed mainly of C18:1, C18:2, and C18:3, that correspond to 84.7% (for soybean) to 95.1% (for canola)

of FAME content. These biodiesels were the least corrosive (Figure 1). Used frying oil, macauba, and palm kernel biodiesels were poorer in C18:1, C18:2, and C18:3, having from 22.0% (for macauba) to 35.1% (for palm kernel) of these esters in their composition. Additionally, they exhibited a high composition of saturated chain esters (45.3 to 66.7%). These biodiesels were the most corrosive (Figure 1).

These results suggest that if, on the one hand, methyl esters of oleic, linoleic and linolenic acids have a negative effect on biodiesel quality by causing a decrease in their oxidative stability,¹² on the other hand, these esters make the biodiesel less corrosive.

Influence of W, AV, and oxidative stability parameters (OSP) on corrosion rate

Although the corrosion rate is apparently well related to the presence of the C18:1, C18:2, and C18:3 esters, the W, AV, and IP of prepared biodiesel (Table 2) should also be considered, since these parameters are related to the corrosivity of the biodiesel.^{9,11-14,16} In order to find out which parameters affect biodiesel corrosiveness, it is important to verify the relationship of the corrosion rate with each of them.

The comparison of the metallic copper corrosion rate *versus* W of biodiesel (Figure 2a) suggests that there is some correlation ($r = -0.50$). Despite being low, two suggestions can be obtained from this correlation coefficient. First, due to the low level of correlation, this parameter could not be considered an important cause of the corrosivity of the investigated biodiesel. Second, paradoxically, by the negative sign of the correlation coefficient, the corrosivity of the biodiesel decreases with the increase of its W as a general trend. This observation disagrees with previous observations where it was found that an increase of W results in more corrosive biodiesel.⁹ However, the corrosion rates are also affected by the other parameters besides W, which could be causing this behavior. A multiple linear regression model may be more appropriate to describe the relationship between W and the corrosion rate.

The correlation between the corrosion rate and AV is shown in Figure 2b. A higher correlation ($r = 0.76$), than was found with the W, was observed. This clearly indicates that AV is an important parameter in the corrosion process under study, as was also found by other researchers.^{10,13,15,16}

IP was employed for evaluating the relationship between the corrosion rate and the oxidative stability of biodiesel. The IP value indicates the effect of the global composition of the biodiesel, including the FAME composition, the FFA contents, water, peroxides, catalysts,

Table 1. Compositional analysis of biodiesels, related oxidative stability parameters (OSP = APE, BAPE, and OX indices), and N_{UNSAT}

FAME	Source oil							
	Used frying oil	Macauba	Palm kernel	Soybean	Corn	Sunflower	Canola	Linseed
C8:0	–	2.15	3.34	–	–	–	–	–
C10:0	–	2.43	3.14	–	–	–	–	–
C12:0	–	43.92	36.52	–	–	–	–	–
C14:0	–	16.88	11.03	–	–	–	–	–
C16:0	8.28	10.14	8.80	10.98	12.20	4.22	4.86	4.90
C16:1	8.35	0.02	0.08	0.09	–	–	–	–
C17:0	8.67	–	0.03	0.09	–	–	–	–
C17:1	8.74	–	0.02	0.05	–	–	–	–
C18:0	9.07	2.26	3.75	3.27	1.60	2.69	–	2.90
C18:1	9.14	19.35	29.68	23.33	36.40	42.80	65.80	31.30
C18:2	9.28	2.65	3.37	54.78	49.80	50.30	22.55	18.90
C18:3	9.44	–	–	6.57	–	–	6.75	42.00
C20:0	9.39	0.12	0.13	0.30	–	–	–	–
C20:1	9.79	0.08	0.11	0.19	–	–	–	–
C22:0	9.85	–	–	0.34	–	–	–	–
APE / (%)	110	44.2	66.5	170	172	186	190	184
BAPE / (%)	28.2	2.65	3.37	67.9	49.8	50.3	36.1	103
OX	0.283	0.0304	0.0396	0.684	0.505	0.512	0.373	1.04
N_{UNSAT}	0.829	0.248	0.366	1.53	1.36	1.43	1.31	1.95

FAME: fatty acid methyl ester; APE: allylic position equivalent; BAPE: bis-allylic position equivalent; OX: oxidability; N_{UNSAT} : number of unsaturated bonds.

Table 2. Water content, acid value, and induction period of the prepared biodiesels

Source oil	Water content / (mg kg ⁻¹)	Acid value / (mg g ⁻¹) ^a	Induction period / h
Sunflower	509 ± 7	0.096 ± 0.004	3.1 ± 0.2
Canola	660 ± 18	0.103 ± 0.002	6.9 ± 0.3
Corn	518 ± 13	0.129 ± 0.003	7.6 ± 0.1
Linseed	809 ± 11	0.15 ± 0.01	2.00 ± 0.01
Used frying oil	385 ± 11	0.17 ± 0.01	1.61 ± 0.02
Soybean	249 ± 4	0.201 ± 0.008	6.0 ± 0.2
Macauba	187 ± 16	0.204 ± 0.008	64.3 ± 0.3
Palm kernel	394 ± 5	0.240 ± 0.003	54 ± 3

^aMilligrams of KOH per gram of biodiesel.

glycerol, methanol, natural antioxidants, etc., on its oxidative stability. To investigate the relationship between biodiesel corrosivity and the oxidative stability related only to the FAME composition, the parameters proposed by Knothe³¹ and Neff *et al.*³² were employed. These authors have demonstrated that the oxidability of biodiesel, in terms of FAME composition, could be estimated by APE (allylic position equivalent), BAPE (bis-allylic position equivalent), and OX (oxidizability) indices, according to equations 2-4 (the first two are written in their generalized form):

$$\text{APE} = ap_a A_{Ca} + ap_b A_{Cb} + ap_c A_{Cc} + \dots \quad (2)$$

$$\text{BAPE} = bp_a A_{Ca} + bp_b A_{Cb} + bp_c A_{Cc} + \dots \quad (3)$$

$$\text{OX} = [0.02(\text{C18:1}) + (\text{C18:2}) + 2(\text{C18:3})]/100 \quad (4)$$

where: ap_x and bp_x are the number of allylic and bis-allylic positions, respectively, in a specific FAME; A_{Cx} is the percentage content of each FAME in biodiesel; C18:1, C18:2, and C18:3 are the percentage content of methyl esters of oleic, linoleic and linolenic acids. The APE, BAPE and OX indices calculated by equations 2-4 are listed in Table 1.

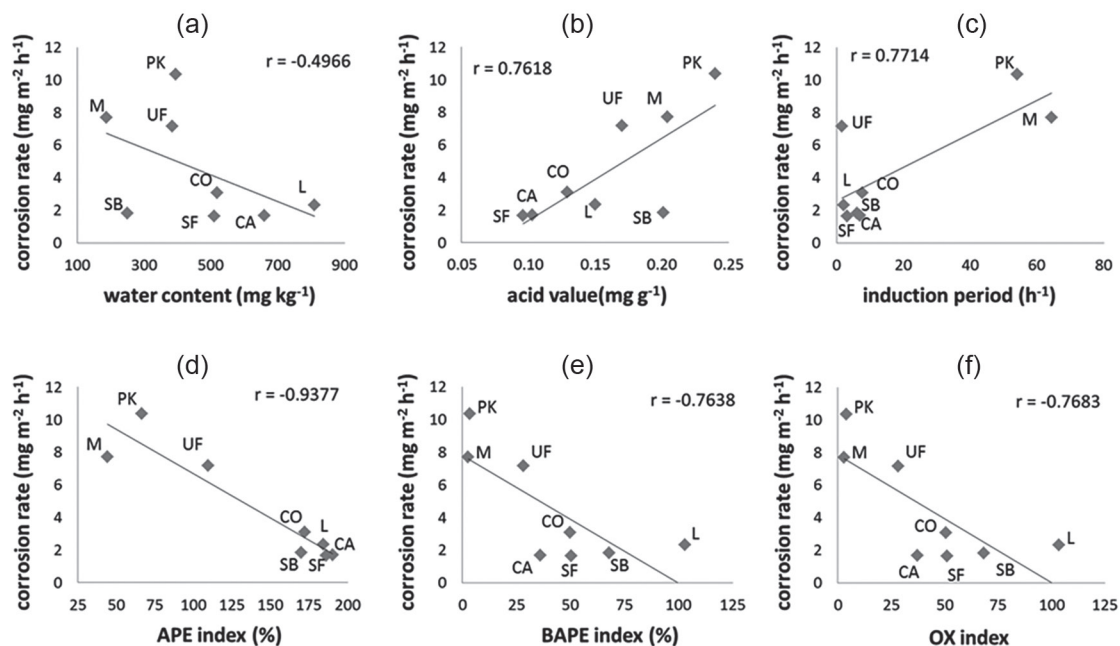


Figure 2. Plots of corrosion rate of metallic copper against: water content (a); acid value (b); induction period (c); APE index (d); BAPE index (e); and OX index (f) of prepared biodiesels. Oil source: soybean (SB), sunflower (SF), corn (CO), canola (CA), linseed (L), palm kernel (PK), macauba (M), and used frying oil (UF).

The relationship between the corrosion rate and the oxidative parameters are shown in Figures 2c-2f. The literature^{10,13,33} has reported that the corrosiveness of biodiesel increases after its oxidation. Therefore, it was expected that the biodiesel with less oxidative stability would be more corrosive as a consequence of the formation of corrosive species during the oxidation process.

Figure 2c shows the relationship between the corrosion rate and the IP of eight different biodiesels. Among them, six (used frying oil (UF), linseed (L), corn (CO), canola (CA), soybean (SB), and sunflower (SF)) present relatively low IP. Among these six, five (L, CO, CA, SB, and SF) present the lowest corrosion rates of the eight studied. Therefore, biodiesels with low IP are less corrosive than those with high IP, demonstrating that the easily oxidizable biodiesels are less corrosive compared to the more stable. Likewise, Figures 2d-2f show that the allylic and bis-allylic carbons (expressed by APE and BAPE contents) and the methyl esters of oleic, linoleic, and linolenic fatty acids (related to OX) inhibit the corrosion, while the literature¹²⁻¹⁴ reports that they favor biodiesel degradation. This behavior can be understood if molecular oxygen reacts preferentially with biodiesel rather than copper, leading to a low corrosion rate for this metal. Inversely, molecular oxygen reacts more rapidly with metallic copper if the biodiesel is more resistant to oxidation.

This is the case, for example, for the biodiesels from palm kernel and macauba oils, which present two of the

three higher IP values observed and also present the two highest rates of corrosion (Figure 2c). On the other hand, the IP of the biodiesel from macauba oil (64.3 ± 0.3 h) was quite different from the IP of the biodiesel from used frying oil (1.61 ± 0.02 h). However, these two biodiesels have very similar corrosiveness (7.7 ± 1.1 vs. 7.17 ± 0.13 $\text{mg m}^{-2} \text{h}^{-1}$). This divergence does not occur in the oxidative stability parameters (OSP) associated with the FAME composition. In such cases, the lowest values of APE, BAPE, and OX indices occur in the three most corrosive biodiesels (from macauba, palm kernel, and used frying oil) (Figures 2d-2f). This fact suggests that the corrosion rate is more closely associated with the FAME composition than with the real biodiesel oxidative stability (measured by the IP value).

The good linear correlation ($r = -0.94$, Figure 2d) of the APE index *versus* corrosion rate demonstrates that allylic carbons must have an important role in the corrosion rate. The reaction of allylic carbons with molecular oxygen dissolved in the biodiesel should decrease the amount of oxygen available to react with the metallic copper, reducing the rate of corrosion. For this reason, the linear correlation coefficient was negative.

It should also be noted that, although the literature relates that bis-allylic carbons are more susceptible to oxidation than allylic carbons,¹⁴ the linear correlation with the BAPE index ($r = -0.76$) was smaller than with the APE index. Indeed, thermodynamically, the bis-allylic carbons are more reactive, but an oxidation process is also subject to kinetic control. Consequently, since the relative

quantity of FAME with allylic carbon is higher than the relative quantity of FAME with bis-allylic carbon (see the APE and BAPE index values, in Table 2), the APE index becomes more relevant than the BAPE index to determine the FAME oxidation and the corrosion process.

As the corrosion rate decreases with the increase of the APE, BAPE and OX indices, which intrinsically are accompanied by an increase in the unsaturation number of the FAME composition, it is reasonable to conclude that unsaturated methyl esters act as sacrificial molecules, protecting the copper against corrosion. The relationship between the OSP associated with FAME composition and the corrosiveness of biodiesel should be the same for any biodiesel that does not suffer an advanced level of oxidation. The oxidation process decreases the level of unsaturation of the esters. This situation leaves molecular oxygen free to react with metallic copper, increasing, therefore, the corrosion rate. Additionally, the short chain acids formed at the end of the biodiesel degradation process will also increase the corrosion of the metal. Therefore, the results presented in this work are in agreement with the literature reports that an increase in the level of oxidation favors corrosion. However, so far as we know, an interesting aspect of the phenomenon of metallic copper oxidation by biodiesel, which has not been reported so far, is the fact that the more easily oxidizable biodiesel is less corrosive towards the metal.

Corrosion rate prediction model

The construction of consistent MLR models can provide mathematical correlations between the corrosion rate of metallic copper and W, AV, and FAME composition, leading to a better understanding of the mechanisms involved in the corrosion process.

When investigating the mechanism of copper corrosion by palm biodiesel, Fazal *et al.*²⁴ proposed that O₂ and H₂O present in the biodiesel would act as causative agents of corrosion, and, in the end, the Cu₂O, CuO, Cu(OH)₂, and CuCO₃ produced are deposited on the metallic surface. Therefore, it is straightforward to expect a relationship between the presence of such compounds and the corrosion rate of metallic copper immersed in the fuel.

The copper surface is in contact mainly with the FAME (saturated and unsaturated), H₂O, and passivating agents (Cu₂O, CuO, Cu(OH)₂ and CuCO₃) deposited on the metal, according to the illustration in Figure 3.

Thus, it is reasonable to assume that the global loss of metallic copper mass is expressed as the sum of the losses of mass that occur in each region of the metal surface in contact with these substances, according to equation 5:

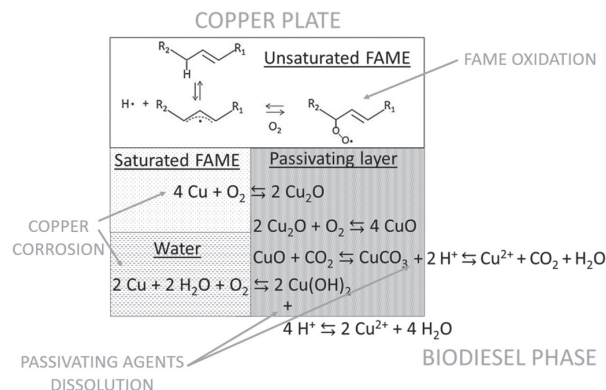


Figure 3. General scheme of a copper plate immersed in biodiesel with FAME (saturated and unsaturated), water, and a passivation layer deposited on the metallic surface. The reactions for corrosion and the formation of passivation agents in each region are in accordance with those proposed by Fazal *et al.*²⁴

$$\Delta m = \Delta m_{\text{H}_2\text{O}} + \Delta m_{\text{pa}} + \Delta m_{\text{FAME}} \quad (5)$$

where: Δm is the global loss of metallic copper mass; $\Delta m_{\text{H}_2\text{O}}$, Δm_{pa} , and Δm_{FAME} are the loss of mass of the copper plate due to contact with water, passivating agents, and FAME, respectively. Considering that O₂ acts in the oxidation process only when dissolved in the liquid phases, the terms $\Delta m_{\text{H}_2\text{O}}$ and Δm_{FAME} encompass this aspect.

The terms of equation 5 can be written as a function of area covered by each substance, according to equations 6-8:

$$\Delta m_{\text{H}_2\text{O}} = c_1 A_{\text{H}_2\text{O}} + b_1 \quad (6)$$

$$\Delta m_{\text{pa}} = -c_2 A_{\text{pa}} + b_2 \quad (7)$$

$$\Delta m_{\text{FAME}} = c_3 A_{\text{FAME}} + b_3 \quad (8)$$

where $A_{\text{H}_2\text{O}}$, A_{pa} , and A_{FAME} are respectively: (i) the surface area of copper in contact with water; (ii) the area of the plate of copper inactivated by passivating agents; (iii) the area of the copper plate in contact with FAME. c_x and b_x are the respective angular and linear coefficients of the equations. The values of b_1 and b_3 are equal to zero, because, theoretically, $\Delta m_{\text{H}_2\text{O}}$ and Δm_{FAME} are equal to zero in absence of water and FAME, respectively. The b_2 coefficient represents the loss of mass when there are no passivating agents ($A_{\text{pa}} = 0$), and should be greater than zero. The negative signal of c_2 is due to the coating of the copper plate by passivating agents decreasing the Δm_{pa} value. If the copper plate is 100% coated by passivating agents, then $\Delta m_{\text{pa}} = 0$.

$\Delta m_{\text{H}_2\text{O}}$ occurs due to water condensation on the metallic surface, and molecular oxygen is the oxidizing agent of the metallic copper (Figure 3).^{10,24} As the surface area of the metallic copper covered by water must be proportional to W, then the equation 6 becomes equation 9. So, W was used to estimate $\Delta m_{\text{H}_2\text{O}}$, and the coefficient c_1' would present a

positive value. The microbial corrosion due to the water condensation may be neglected due to the high immersion test temperature (60 °C), which killed the microbes.

$$\Delta m_{H_2O} = c_1'W + b_1' \quad (9)$$

The passivating agents deposited on the metal in the form of copper compounds (Cu_2O , CuO , $Cu(OH)_2$ and $CuCO_3$) inhibit corrosion. The area covered by passivation agents (A_{pa}) may be related to AV, because the free acid in biodiesel may promote the dissolution of the passivating agents (Figure 3), and the copper will be less protected by the passivation layer becoming more susceptible to corrosion. An increase of AV will decrease A_{pa} and, consequently, Δm_{pa} will be higher. Thus, equation 7 becomes equation 10 and the c_2' coefficient would be positive.

$$\Delta m_{pa} = c_2'AV + b_2' \quad (10)$$

The mass loss of the metallic copper surface in contact with FAME, Δm_{FAME} , must be related to FAME composition, being caused by molecular oxygen (Figure 3). Two terms could be used to estimate Δm_{FAME} , according to the following discussions: number of unsaturated bonds (N_{UNSAT}) in biodiesel or the concentration of O_2 available to attack the copper plate.

Unsaturated bonds contribute to the adsorption of corrosion inhibitors on the metallic surface, protecting the metal against the corrosion caused by acid attack.³⁴ Similarly, unsaturated FAME could be adsorbed on a copper surface, protecting it against corrosion, and the O_2 will react preferentially with the allylic or bis-allylic carbons (Figure 3). Corrosion will occur in the region of the surface of the copper plate that is in contact with saturated FAME (Figure 3). In this case, only a fraction of A_{FAME} will undergo O_2 attack. Thus, equation 8 could best be written as:

$$\Delta m_{FAME} = c_3A_{SFAME} + b_3 \quad (11)$$

where A_{SFAME} is the area covered by saturated FAME and b_3 , as in equation 8, is equal to zero. Equation 8 can also be written as a function of the area covered by unsaturated FAME (A_{UFAME}) becoming:

$$\Delta m_{FAME} = c_3A_{UFAME} + b_3 \quad (12)$$

The coefficient c_3 will be negative because coating the copper plate will decrease the mass loss. In equation 12, the linear coefficient b_3 will be greater than zero and equal to Δm_{FAME} when there is no unsaturated FAME. The area

covered by unsaturated FAME must be directly proportional to N_{UNSAT} in biodiesel and equation 12 becomes:

$$\Delta m_{FAME} = -c_3'N_{UNSAT} + b_3' \quad (13)$$

N_{UNSAT} can be calculated according equation 14:

$$N_{UNSAT} = (n_aA_a + n_bA_b + n_cA_c + \dots)/100 \quad (14)$$

where n_x is the unsaturation number of a specific FAME, and A_x is the percentage content of each FAME in biodiesel. The N_{UNSAT} values are listed in Table 1.

The adsorption of molecules on the metal surface is well related in unsaturated chains with conjugated double bonds,³⁵ which is not the case with the methyl esters that constitute the biodiesels used (Table 1). Therefore, it is also possible that the unsaturated FAME is not well adsorbed onto the surface of the copper plate and equations 11, 12, and 13 are not valid. In this case, Δm_{FAME} could be correlated to the O_2 available to oxidize the copper plate. If biodiesel is hardly oxidized, more O_2 will be available to react with the metal, increasing the corrosion rate, in comparison to more easily oxidized biodiesel. On the contrary, if the biodiesel presents high oxidability, the O_2 will react with the FAME to a greater extent, and, consequently, the copper plate will be less corroded. As the oxidability of biodiesel is related to IP and to the APE, BAPE, and OX indices (here generalized as OSP), Δm_{FAME} could be written as a function of these parameters according to equations 15 and 16, instead of the area of the copper surface covered by FAME (A_{FAME}) previously described by equation 8.

$$\Delta m_{FAME} = c_4IP + b_4 \quad (15)$$

$$\Delta m_{FAME} = -c_5OSP + b_5 \quad (16)$$

In equation 15, c_4 is positive, because the increase of the IP value is related to the decrease of FAME oxidation. Consequently, the O_2 present will be more available to react with copper, increasing the mass loss of the plate. In the correlation expressed by equation 16, c_5 is negative, because FAME oxidation increases with an increase of the OSP value, leaving less O_2 available to react with copper. Consequently, a decrease of the Δm_{FAME} will be observed.

In accordance with the previous considerations, the mass loss (Δm) in equation 5 can be written, according to equations 17, 18 and 19, as a function of W, AV, N_{UNSAT} , IP, and OSP:

$$\Delta m = c_1'W + c_2'AV - c_3'N_{UNSAT} + (b_1' + b_2' + b_3') \quad (17)$$

$$\Delta m = c_1'W + c_2'AV - c_4IP + (b_1' + b_2' + b_4) \quad (18)$$

$$\Delta m = c_1'W + c_2'AV - c_5OSP + (b_1' + b_2' + b_5) \quad (19)$$

Replacing Δm of equation 1 by equations 17-19 and holding the A and t parameters constant, equations 20, 21 and 22 can be proposed:

$$\text{corrosion rate} = a_W W + a_{AV} AV - a_N N_{\text{UNSAT}} + o \quad (20)$$

$$\text{corrosion rate} = a_W W + a_{AV} AV + a_{IP} IP + p \quad (21)$$

$$\text{corrosion rate} = a_W W + a_{AV} AV - a_{OSP} OSP + q \quad (22)$$

where a_W , a_{AV} , a_N , a_{IP} and a_{OSP} are the respective coefficients of corrosion related to each parameter (they will have the same signs as c_1' , c_2' , c_3' , c_4 and c_5 , respectively, as discussed above); o , p , and q are the linear coefficients from the sum of the b_1' , b_2' , b_3' , b_4 and b_5 coefficients, according to equations 17-19. All coefficients of equations 20-22 can be determined empirically by multiple linear regression.

Table 3 shows the MLR models obtained by combining the parameters of equations 20-22. Additionally, a prediction model was created using only the APE index (without W and AV), because this parameter gave the best linear correlation with the corrosion rate (Figure 2d). The predicted and experimental corrosion rate values are shown in Table 4.

As can be seen from Table 3, the use of IP as an oxidative stability parameter gave a weaker model (model 2)

than those with oxidation parameters related to FAME composition (models 3-6) and to the N_{UNSAT} (model 1). Model 2 presents no statistically significant predictive capability at significance level of 0.05 (F -value < 0.05).

In the other MLR models (1, 3, 4, and 5), all variables related to the FAME composition (N_{UNSAT} , APE, BAPE, and OX, respectively) present a statistically significant predictive capacity at significance level of 0.05 (p -values < 0.05 , see Table 5) in relation to the other independent variables (W and AV). The same trend was observed for AV in models 1, 4, and 5.

The W variable, on the other hand, did not present statistically significant predictive capacity in any model (p -values > 0.05 , Table 5), but this does not mean that water is not an agent of corrosion. The amount of water is substantially lower in biodiesel than the amount of FAME. Therefore, the area of the copper plate in contact with water is very small. Consequently, the predictive capacity of the model related corrosion caused by W becomes statistically insignificant.

These results reinforce the idea that the parameters more strictly related to the oxidizable fatty chain content, and, ultimately, unsaturated chains, are more important than the IP value and W for the corrosion rate. AV is also relevant;

Table 3. Models of linear regression constructed using W , AV , N_{UNSAT} , IP , and OSP (APE, BAPE and OX indices)

Model	Equation (corrosion rate =)	R-multiple	R-squared	Standard error	F -value
1	$0.006W + 31.34AV - 4.97N_{\text{UNSAT}} - 2.27$	0.97	0.94	1.12	0.007
2	$0.001W + 31.22AV + 0.065IP + 2.27$	0.84	0.70	2.48	0.159
3	$0.004W + 10.15AV - 0.058APE + 8.93$	0.96	0.92	1.28	0.012
4	$0.007W + 47.53AV - 0.073BAPE - 3.14$	0.95	0.89	1.47	0.020
5	$0.007W + 47.28AV - 7.37OX - 3.060$	0.95	0.90	1.45	0.019
6	$-0.055APE + 12.14$	0.94	0.88	1.28	0.001

W : water content; AV : acid value; N_{UNSAT} : number of unsaturated bonds; IP : induction period; APE: allylic position equivalent; BAPE: bisallylic position equivalent; OX: oxidability.

Table 4. Corrosion rates predicted by linear regression models and experimental values

Biodiesel	Predicted corrosion rate / ($\text{mg m}^{-2} \text{h}^{-1}$)						Experimental corrosion rate / ($\text{mg m}^{-2} \text{h}^{-1}$)
	Model 1	Model 2	Model 3	Model 4	Model 5	Model 6	
Sunflower	1.19	1.50	1.35	1.09	1.09	1.98	1.65
Canola	2.99	2.13	1.86	3.46	3.45	1.76	1.68
Corn	2.65	2.83	2.53	2.76	2.76	2.73	3.09
Linseed	2.24	3.45	3.34	1.79	1.79	2.08	2.33
Used frying oil	5.72	3.57	6.01	5.41	5.45	6.16	7.17
Soybean	2.34	4.67	2.20	3.09	3.06	2.86	1.84
Macauba	8.40	8.48	9.26	7.60	7.60	9.72	7.71
Palm kernel	10.27	9.17	9.25	10.61	10.62	8.51	10.35

Table 5. *p*-Values of independent variables for models 1-6

Model	Variable						
	W	AV	N _{UNSAT}	IP	APE	BAPE	OX
1	0.099	0.049	0.0084	–	–	–	–
2	0.86	0.32	–	0.28	–	–	–
3	0.24	0.54	–	–	0.015	–	–
4	0.18	0.027	–	–	–	0.026	–
5	1.7	0.026	–	–	–	–	0.025
6	–	–	–	–	0.00058	–	–

W: water content; AV: acid value; N_{UNSAT}: number of unsaturated bonds; IP: induction period; APE: allylic position equivalent; BAPE: bisallylic position equivalent; OX: oxidability.

however, as the influence of the APE index is highlighted, the AV variable does not present a statistically significant predictive capacity in model 3 (*p*-value > 0.05, Table 5). Because of this, model 6 has a high predictive capacity in comparison to other models (Table 3).

The proposed models presented in Table 3 are not presented with the intention of employing them as an alternative for the prediction of corrosion rates, even though they may be used for this purpose (except model 2). The immersion tests are simpler and cheaper for the determination of corrosion rate than the required methods for the determination of W, AV, IP, and FAME composition for the prediction of corrosion rates by the proposed models. However, an important aspect of these models should be highlighted: all the signs of the independent variable coefficients, N_{UNSAT} (–), IP (+), APE (–), BAPE (–), OX (–), W (+), and AV (+), are in accordance with those previously predicted for coefficients a_1 - a_3 of equations 20-22. This fact supports the proposed description of the main phenomena that govern the corrosive process which occurs on the metallic copper surface and in the biodiesel phase (Figure 3).

Therefore, MLR models 3-5 present special interest as they clearly suggest that the oxidative stability, W, and AV are directly related to the corrosion rate mechanism. These models also indicate that the APE, BAPE, and OX indices decrease the corrosion rate on the copper plate as they compete for the O₂ present in the biodiesel due to their own oxidation processes. In parallel, the good fit of the corrosion rate with experimental values obtained by model 1 (Table 3 and 4) also suggests that unsaturated FAME protects the copper plate against O₂ attack due to its own adsorption on the metallic surface.

Conclusions

Biodiesel corrosivity is related to the content of methyl esters of oleic (C18:1), linoleic (C18:2) and

linolenic (18:3) acids, more specifically the levels of unsaturated methyl esters. Biodiesels with low IP were less corrosive than those with high IP, demonstrating that easily oxidizable biodiesels are less corrosive than the less oxidizable ones. Likewise, allylic and bis-allylic carbons (expressed by APE and BAPE indices) inhibit the corrosion, although they favor the oxidation of biodiesel. A higher correlation between corrosion rate and AV was also observed, which indicates that AV is an important parameter in the corrosion process.

The prediction models that relate the corrosion rate variable to the average unsaturation number, parameters of oxidative stability, AV, and W can explain the corrosion of metallic copper caused by biodiesel. More easily oxidizable biodiesel is less corrosive than hardly oxidizable biodiesel, because the dissolved O₂ should react with unsaturated FAME, which would adsorb on the copper surface acting as “sacrificial molecules” to protect the copper against corrosion. The water condensed on the metallic surface will promote copper oxidation due to the dissolved O₂, but the predictive capacity of the corrosion rate related to W is statistically insignificant because of the low amount of water in biodiesel in comparison to the amount of FAME. Although the corrosion reaction progressively produces a passivation layer on the copper surface, free acids will react with these byproducts, preventing a decrease of the exposed surface area of the metal and, consequently, avoiding a decrease in the rate of corrosion.

Acknowledgments

This study was financed in part by the Coordenação de Aperfeiçoamento de Pessoal de Nível Superior (CAPES, Brazil), finance code 001, and by the Conselho Nacional de Desenvolvimento Científico e Tecnológico (CNPq, Brazil), finance codes 404808/2013-1, 420868/2016-0 and 304605/2016-6.

References

1. Meher, L. C.; Sagar, D. V.; Naik, S. N.; *Renewable Sustainable Energy Rev.* **2006**, *10*, 248.
2. Damanik, N.; Ong, H. C.; Tong, C. W.; Mahlia, T. M. I.; Silitonga, A. S.; *Environ. Sci. Pollut. Res.* **2018**, *25*, 15307.
3. Sirviö, K.; Heikkilä, S.; Help, R.; Niemi, S.; Hiltunen, E.; *Agron. Res.* **2018**, *16*, 1237.
4. Chandran, D.; Kiat, N. G.; Nang, H. L. L.; Suyin, G.; Choo, Y. M.; Jahis, S.; *J. Oil Palm Res.* **2016**, *28*, 64.
5. Haryono, I.; Ma'ruf, M.; Setiaprada, H.; *Int. J. Energy Environ.* **2016**, *7*, 383.
6. EN 16709:2015: *Automotive Fuels - High FAME Diesel Fuel (B20 and B30) - Requirements and Test Methods*, European Committee for Standardization, Brussels, Belgium, 2015.
7. Conselho Nacional de Política Energética (CNPE); *Estabelece a Adição Obrigatória, em Volume, de Dez por Cento de Biodiesel ao Óleo Diesel Vendido ao Consumidor Final*; Resolução CNPE No. 23 2017, de 09.11.2017, available at <http://www.mme.gov.br>, accessed on April 25, 2019.
8. Haseeb, A. S. M. A.; Masjuki, H. H.; Ann, L. J.; Fazal, M. A.; *Fuel Process. Technol.* **2010**, *91*, 329.
9. McCormick, R. L.; Ratcliff, M.; Moens, L.; Lawrence, T.; *Fuel Process. Technol.* **2007**, *88*, 651.
10. Fazal, M. A.; Haseeb, A. S. M. A.; Masjuki, H. H.; *Fuel Process. Technol.* **2010**, *91*, 1308.
11. Ahmmad, M. S.; Hassan, M. B. H.; Kalam, M. A.; *Int. J. Green Energy* **2018**, *15*, 393.
12. Zuleta, E. C.; Baena, L.; Rios, L. A.; Calderón, J. A.; *J. Braz. Chem. Soc.* **2012**, *23*, 2159.
13. Pullen, J.; Saeed, K.; *Renewable Sustainable Energy Rev.* **2012**, *16*, 5924.
14. Knothe, G.; Dunn, R. O.; *J. Am. Oil Chem. Soc.* **2003**, *80*, 1021.
15. Niczke, L.; Czechowski, F.; Gawel, I.; *Prog. Org. Coat.* **2007**, *59*, 304.
16. Tsuchiya, T.; Shiotani, H.; Goto, S.; Sugiyama, G.; Maeda, A.; *SAE [Tech. Pap.]* **2006**, *01*, 3303.
17. Singha, B.; Korstad, J.; Sharma, Y. C.; *Renewable Sustainable Energy Rev.* **2012**, *16*, 3401.
18. Haseeb, A. S. M. A.; Fazal, M. A.; Jahurul, M. I.; Masjuki, H. H.; *Fuel* **2011**, *90*, 922.
19. Sylvester O.; Adams, F. V.; Okoro, L. N.; *Int. J. Sci. Eng. Res.* **2015**, *6*, 546.
20. Sorate, K. A.; Bhale, P. V.; *J. Sci. Ind. Res.* **2012**, *72*, 48.
21. Kaul, S.; Saxena, R. C.; Kumar, A.; Negi, M. S.; Bhatnagar, A. K.; Goyal, H. B.; Gupta, A. K.; *Fuel Process. Technol.* **2007**, *88*, 303.
22. Sgroi, M.; Bollito, G.; Saracco, G.; Specchia, S.; *J. Power Sources* **2015**, *149*, 8.
23. Geller, D. P.; Adams, T. T.; Goodrum, J. W.; Pendergrass, J.; *Fuel Process. Technol.* **2008**, *87*, 92.
24. Fazal, M. A.; Haseeb, A. S. M. A.; Masjuki, H. H.; *Corros. Sci.* **2013**, *67*, 50.
25. Aquino, I. P.; Hernandez, R. P. B.; Chicoma, D. L.; Pinto, H. P. F.; Aokia, I. V.; *Fuel* **2012**, *102*, 795.
26. Sarin, A.; Arora, R.; Singh, N. P.; Sharma, M. P.; Malhotra, R. K.; *Energy* **2009**, *34*, 1271.
27. EN 14112:2003: *Fat and Oil Derivatives - Fatty Acid Methyl Esters (FAME); Determination of Oxidation Stability (Accelerated Oxidation Test)*, European Committee for Standardization, Brussels, Belgium, 2003.
28. EN ISO 12937:2000: *Petroleum Products - Determination of Water-Coulometric Karl Fischer Titration Method*, European Committee for Standardization, Brussels, 2000.
29. Aricetti, J. A.; Tubino, M.; *Fuel* **2012**, *95*, 659.
30. ASTM G1-03: *Standard Practice for Preparing, Cleaning, and Evaluating Corrosion Test Specimens*, ASTM International, West Conshohocken, PA, 2003.
31. Knothe, G.; *J. Am. Oil Chem. Soc.* **2002**, *79*, 847.
32. Neff, W. E.; Selke, E.; Mounts, T. L.; *J. Am. Oil Chem. Soc.* **1992**, *69*, 111.
33. Kumar, N.; *Fuel* **2017**, *190*, 328.
34. Kumari, P. P.; Shetty, P.; Rao, S. A.; *Arabian J. Chem.* **2017**, *10*, 653.
35. Alobaidy, A.; Kadhum, A.; Al-Baghdadi, S.; Al-Amiery, A.; Kadhum, A.; Yousif, E.; Mohamad, A.; *Int. J. Electrochem. Sci.* **2015**, *10*, 3961.

Submitted: December 20, 2018
Published online: April 30, 2019

